IEICE TRANS. COMMUN., VOL.E84–B, NO.7 JULY 2001

PAPER *Special Issue on Adaptive Array Antenna Techniques for Advanced Wireless Communications*

Field Test Results for a Beam and Null Simultaneous Steering S/T-Equalizer in Broadband Mobile Communication Environments

Takahiro ASAI[†], **Shigeru TOMISATO**[†], *and* **Tadashi MATSUMOTO**[†], ***Regular Members***

SUMMARY This paper proposes a beam and null simultaneous steering Space-Time Equalizer (S/T-Equalizer). The proposed S/T-Equalizer performs separated S/T-signal processing in order to reduce computational complexity to a practical level. For spatial signal processing, a new Adaptive Array Antenna algorithm is used that combines the beam and null steering concepts. For temporal signal processing, a conventional delayed decision feedback sequence estimation equalizer may be used. The proposed S/T-Equalizer was prototyped, and a series of field tests was conducted using a 5 GHz frequency band to evaluate transmission performances of the proposed system. Results show that the proposed S/T-Equalizer can reduce inter-symbol interference effects while maintaining reasonable signal strength, thereby improving BER performance.

key words: *broadband mobile communication, multipath fading, adaptive array antenna, adaptive equalizer*

1. Introduction

Mobile multimedia communications demand the creation of broadband signal transmission techniques that offer transmission rates of several tens of Mbps. These techniques must overcome problems such as Co-Channel Interference (CCI) and Inter-Symbol Interference (ISI) as well as relatively large propagation loss inherent to broadband mobile communications. Joint Space/Time-Equalization (S/T-Equalization) is considered most effective in reaching these goals [1], [2]. S/T-Equalization is a unified concept combining conventional adaptive array antennas (AAAs) and temporal equalizers (TE). Temporal equalizers aim to reduce ISI and combine delayed desired signal components, while AAAs suppress CCI and enhance antenna gain towards the desired signal's incident angle. Optimal performance can be achieved through two-dimensional (joint spatial and temporal) optimization of the S/T-Equalizer's parameters [3]. Unfortunately, it is prohibitively complex in many cases to implement the optimal S/T-Equalizer, and a technique that significantly reduces the complexity is required.

This paper proposes a new suboptimal S/T-Equalization technique that separates spatial and temporal signal processing. This separation reduces the computational complexity of signal processing to a practical level, however, requires the separated spatial equalizer to obtain spatial reference of incident signals. Fortunately, the spatial reference does not change as fast as channel fading variation, and therefore, it can be fixed over not a too long period of time. The MUSIC algorithm may be used to obtain spatial reference. A new AAA algorithm is proposed for spatial equalization. The proposed algorithm combines the beam and null steering concepts; a sharp beam is steered towards the desired signal while nulls are steered towards interferers. The AAA is followed by a temporal equalizer. Although any form of equalizer can be used for temporal equalization, the Delayed Decision Feedback Sequence Estimation (DDFSE) equalizer may be a good choice [4] since it offers a reasonable tradeoff between performance and complexity.

The proposed S/T-Equalizer was prototyped. A series of field tests was then conducted in a 5 GHz frequency band to evaluate signal transmission performance of the prototyped system. It took approximately 100 ms for the prototyped system to run the MUSIC algorithm for 8-element antenna array, which is not a heavy burden in terms of computational complexity.

2. Configuration of S/T-Equalizer

Figure 1 shows a block diagram of the proposed S/T-Equalizer. Parameter Estimator-1 (PE-1) performs spatial signal processing for the proposed beam and null steering AAA algorithm, and Parameter Estimator-2

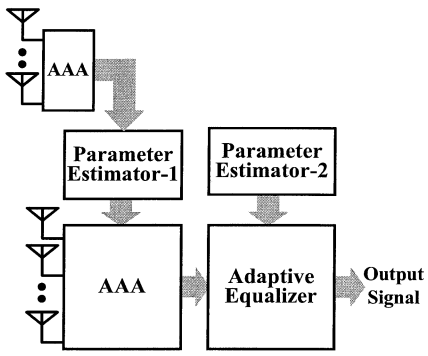

Fig. 1 Configuration of proposed S/T-Equalizer.

Manuscript received November 27, 2000.
Manuscript revised February 13, 2001.

[†]The authors are with Wireless Laboratories, NTT DoCoMo, Inc., Yokosuka-shi, 239-8536 Japan.

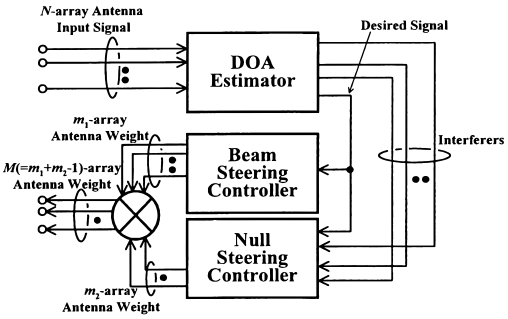

Fig. 2 Configuration of Parameter Estimator-1.

(PE-2) performs temporal signal processing for temporal equalization, both take run independently of the other.

2.1 Spatial Equalization

The proposed AAA algorithm first estimates the direction-of-arrival (DOAs) of incident signals. It then forms a beam pattern based on the DOA estimates: a sharp beam is steered towards the desired signal and nulls towards other signals. Figure 2 shows a detailed configuration of PE-1. The DOA estimator in Fig. 2 uses a super-resolution algorithm to estimate DOAs and powers of signals impinging on an N-element array antenna. The MUSIC algorithm [5] may be used for DOA estimation. The simple classification used here is that the strongest of the detected signals is the desired signal, and the others are the interferers. This classification is reasonable in relatively simple propagation environments. In the presence of both multi-path and interference components, the strongest signal detected may not be the signal that should be detected but indeed may be the one that should be suppressed. In such complex environments, the true desired signal could be determined with the help of a higher layer of the system control. For example, periodic transmission of relatively long unique word sequence and its correlation detection may be used to suppress interference components even if their received strengths are larger than the desired signal's

Let DOA of the desired signal be denoted by θ_0, and DOAs of interferers by θ_i $(1 \leq i \leq L-1)$, where L is the number of signals detected by the DOA estimator. Let σ_0^2 denote the detected desired signal power, and σ_i^2 $(1 \leq i \leq L-1)$ the powers of the others. The M-element array antenna's weight vector can be calculated by using θ_i $(0 \leq i \leq L-1)$ and σ_i^2 $(0 \leq i \leq L-1)$ so that it forms a beam steered towards the desired signal while forming nulls towards the interferers.

Let $\boldsymbol{c} = (c_1, c_2, \cdots, c_{m_1})^T$ denote the m_1-element array antenna's weight distribution that forms a specific beam pattern. The Taylor or Chebyshev distributions may be used as $\boldsymbol{c}$. It follows that the m_1-element array antenna's weight vector for beam steering, $\boldsymbol{W}_{beam}$, can be calculated by using θ_0 of the desired signal's DOA as

$$\boldsymbol{W}_{beam} = (c_1 s_{b,1}(\theta_0), c_2 s_{b,2}(\theta_0), \cdots, c_{m_1} s_{b,m_1}(\theta_0))^T, \quad (1)$$

where $\boldsymbol{s}_b(\theta_0) = (s_{b,1}(\theta_0), s_{b,2}(\theta_0), \cdots, s_{b,m_1}(\theta_0))^T$ is the steering vector for θ_0.

An m_2-element array antenna's weight vector for null steering, $\boldsymbol{W}_{null}$, can be calculated by using the DOAs of the desired signal and the interferers. If the number of interferers $(L-1)$ is larger than the null steering array antenna's degree-of-freedom $m_2 - 1$, not all the interferers can be canceled. In such cases, the $m_2 - 1$ strongest interferers are selected and canceled. In order to calculate the array antenna's weight vector that has nulls towards $m_2 - 1$ interferers, the Howell-Applebaum algorithm [6] can be used. The array correlation matrix $\boldsymbol{R}$ is defined as;

$$\boldsymbol{R} = \sum_{i=1}^{m_2-1} \sigma_i^2 \boldsymbol{s}_n(\theta_i) \boldsymbol{s}_n{}^{\boldsymbol{H}}(\theta_i) + \sigma^2 \boldsymbol{I}_{m_2}, \quad (2)$$

where $\boldsymbol{s}_n(\theta_i)$, σ_i^2, and σ^2 represent the m_2-element steering vectors associated with the directions θ_i $(1 \leq i \leq m_2 - 1)$, powers of interferers and noise, respectively. $\boldsymbol{I}_{m_2}$ denotes an $m_2 \times m_2$ unit matrix.

The null steering array antenna's weight vector $\boldsymbol{W}_{null}$ can then be expressed as

$$\boldsymbol{W}_{null} = \boldsymbol{R}^{-1} \boldsymbol{s}_n(\theta_0), \quad (3)$$

where $\boldsymbol{s}_n(\theta_0)$ represents the m_2-element steering vector associated with the direction θ_0[†]. An M $(= m_1 + m_2 - 1)$-element array antenna's weight vector for beam and null steering can finally be obtained from $\boldsymbol{W}_{beam}$ and $\boldsymbol{W}_{null}$ as

$$\boldsymbol{W} = \boldsymbol{W}_{beam} * \boldsymbol{W}_{null}, \quad (4)$$

where $*$ denotes a convolution between the two vectors (See in Appendix). To apply Eq. (4) properly, the array has to satisfy the rotational invariance condition [7] such as linear arrays having equal element spacing. Equation (4) can be folded into $\boldsymbol{W} = \boldsymbol{B}\boldsymbol{W}_{null}$, where matrix $\boldsymbol{B}$ is given by

$$\boldsymbol{B} = \begin{bmatrix} w_{b,1} & 0 & \cdots & 0 \\ w_{b,2} & w_{b,1} & \cdots & 0 \\ \vdots & \vdots & & \vdots \\ w_{b,m_1} & w_{b,m_1-1} & \cdots & 0 \\ 0 & w_{b,m_1} & \cdots & 0 \\ 0 & 0 & \cdots & 0 \\ \vdots & \vdots & & \vdots \\ 0 & 0 & \cdots & w_{b,1} \\ 0 & 0 & \cdots & w_{b,2} \\ \vdots & \vdots & & \vdots \\ 0 & 0 & \cdots & w_{b,m_1} \end{bmatrix}. \quad (5)$$

[†]In the prototyped system, Sample Matrix Inversion (SMI) algorithm was used to caluculate $\boldsymbol{W}_{null}$.

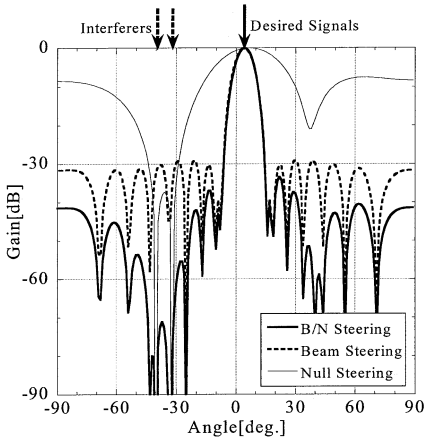

Fig. 3 An example of the beam pattern obtained by computer simulation.

Figure 3 shows a typical beam pattern obtained as a simulation result for the proposed algorithm, where three signals are assumed to have been impinging on the antenna. The thick, thin, and dashed lines represent the beam patterns corresponding to $\boldsymbol{W}$, $\boldsymbol{W}_{beam}$, and $\boldsymbol{W}_{null}$, respectively. The beam pattern with $\boldsymbol{W}$ inherits both $\boldsymbol{W}_{beam}$ and $\boldsymbol{W}_{null}$'s designed beam patterns: the sharp main beam is steered towards the desired signal's DOA θ_0 and the nulls towards the interferers.

In the presence of interferers, the desired received signal may not have the largest strength (As described in Sect. 2.1, the desired signal's DOA can be determined with the help of a higher layer of the system control). Since both the desired and interference signal's strength vary due to fading, of which range reaches over 40 dB, the 30 dB sidelobe suppression is not sufficient. The proposed beam and null simultaneous steering algorithm can further suppress the interference components.

2.2 Temporal Equalization

Even though the spatial equalizer with the proposed beam and null steering algorithm can eliminate the effects of interference and most of the delayed desired signal components, some of the delayed desired signal components, having incident angles very close to the desired signal, may also be captured by the main beam. These components cause ISI distortion on the received desired signal at the output of the spatial equalizer. The primary purpose of the temporal equalizer following the spatial equalizer is to eliminate the ISI caused by the delayed desired signal components captured by the main beam.

For temporal equalization, Maximum Likelihood Sequence Estimation (MLSE) equalizers [8] are known to achieve optimal performance. Unfortunately, the computational complexity of MLSE equalizers is exponential to the delay spread on the received desired signal, and hence it is impractical to use MLSE in ISI-rich broadband mobile communication environments. Therefore, some type of complexity-reduced sub-optimal detector is needed for temporal equalization.

Table 1 Specification of prototyped system.

Frequency band	5 GHz
Duplexing	FDD (70 MHz separation)
Modulation	GMSK
Baudrate	14 Mbps
Bit-rate	1.9 Mbps
Packet length	1536 symbols
Multiplexing	4-slot-TDM
Adaptive Array Antenna	
DOA Estimation(N)	8 element array
Algorithm	MUSIC (without spatial smoothing)
Beamforming (M)	19 element linear array
Beam Steering(m_1)	16 elements Taylor distribution
Null Steering(m_2)	4 elements
Temporal Equalizer	15-tap DDFSE (MLSE:4, DFE:11)

2.3 Timing Control

If the taps of the spatial and temporal equalizers are changed asynchronously, updating the spatial equalizer taps may interfere with the signal reception using the temporal equalizer. Hence, spatial and temporal signal processing should be separated such that the equalizers can update their taps independently. An advantage of the DOA-based spatial equalizer is that DOAs of the incident signals basically stay constant over several milliseconds, which corresponds to a couple of data frames. Hence the spatial equalizer taps can be kept constant over a couple of frames, while those of the temporal equalizer have to be updated frame-by-frame. This allows, without causing severe performance degradation, the taps of the spatial equalizer to be updated in the gap between frames. The proposed separated S/T-Equalizer utilizes this concept, and so demands timing control of operation.

3. Field Test Results

3.1 Specification of Prototyped System

The proposed S/T-Equalizer was prototyped for 4-slot-TDM GMSK signal transmission. Each slot was made of a 450-bit preamble, 1536-bit information segment, and several bits of overhead. The signal transmission baudrate was 14 Mbps. However, because of the overhead for some implementation purposes, effective information bit rate per a slot is about 1.9 Mbps. 5.165 GHz and 5.235 GHz were used for up- and downlinks, respectively, in duplexing the channels. A series of field tests was conducted using the prototyped system. Table 1 summarizes major specifications of the

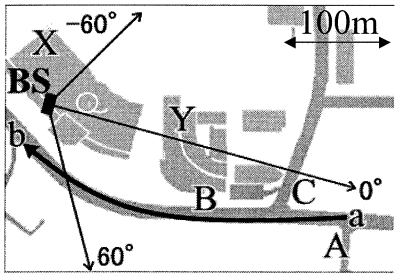

Fig. 4 Measurement course for field tests.

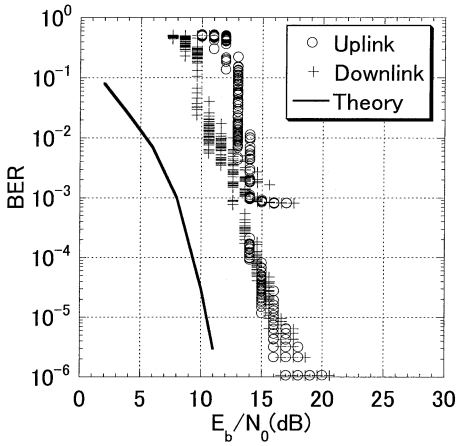

Fig. 5 BER performances at Point A.

prototyped system. A linear array antenna with a minimum element spacing of half the wavelength was used. For DOA estimation, an 8-element linear array was used. The MUSIC algorithm was run on the prototyped system using the 8-element linear array output vector to detect DOAs. A 19-element linear array, which was located separately from but close enough in space to the DOA detector's 8-element array, was used for beamforming. Of the 19 antenna elements, 16 were used for beam steering and 4 for null steering, which satisfies $m_1 + m_2 - 1 = M$. Taylor distribution was used as the array antenna's weight distribution for beam steering. The received signals are combined by using the calculated antenna weights in the RF domain to avoid the inevitable losses incurred by RF/IF circuitry. The algorithm for the spatial signal processing was implemented by using ASIC (Application Specific Integrated Circuit) and FPGA (Field Programable Gate Array) chips. Time for running MUSIC algorithm with 256 snapshots for 8-element linear array is less than 100 ms.

For temporal equalization, a DDFSE equalizer [4] was used. The DDFSE equalizer combines the concepts of the MLSE equalizer and the Decision Feedback Equalizer (DFE); by eliminating some of the MLSE states from the trellis diagram for the channel, its complexity remains feasible. The DDFSE equalizer has two sets of taps: one for MLSE, the other for DFE. In the prototyped system, MLSE has 4 taps and DFE 11 taps, resulting in 15 taps in total, which, with the symbol duration T, covers delay spread of up to 14 T. In addition to signal detection, the temporal equalizer also outputs an estimate of the delay profile as a result of channel estimation. The algorithm for the temporal signal processing was implemented by using FPGA chips to support 1.9 Mbps effective information bit rate.

3.2 Filed Test Courses

A series of field tests was conducted to evaluate signal transmission performance of the prototyped system. Figure 4 shows the measurement course for the field tests. As a Base Station (BS), the prototyped proposed S/T-Equalizer was located on the top of Building X to receive the signal transmitted from a Mobile Station (MS). BS antenna height was about 20 m†. An omnidirectional monopole antenna was located on the top of the vehicle, and used for signal transmission and reception at the vehicle. For downlink signal transmission from the BS, the beam pattern obtained as a result of the uplink signal reception was used. This is reasonable, considering the 70 MHz frequency separation in duplexing the uplink and downlink channels at the 5 GHz band (See Table 1). Points A has Line-Of-Sight (LOS) paths: other locations are non LOS (NLOS) regions due to the presence of Buildings X and Y.

3.3 BER and PER Performances under LOS Conditions

BER performance was first evaluated with the MS located at Point A (See Fig. 4). The DOA estimator detected only a single path having 10 degree DOA, which corresponds to the look angle from the BS to Point A. Figure 5 shows measured BERs of the S/T-Equalizer versus received E_b/N_0, where E_b is defined as signal power at the array output after combining with calculated antenna weights††. In order to change the E_b/N_0 value, the transmission power was controlled. The solid line represents the theoretical BER curves under 1-path static channel. Delay spread estimated by the tempo-

†The proposed S/T-Equalizer separates spatial and temporal signal processing based on the assumption that DOAs of incident signals vary slowly. This assumption is satisfied when BS antenna is located on top of a relatively tall building and the density of obstacles is relatively low. Due to the limitations in availabe BS antenna installation space and transmitter power, the field test was conducted in the area of about 400 m radius which included non Line-Of-Sight (NLOS) regions.

††In this case, the BER/PER curves shown in this paper should not necessarily be understood as overall performances of the proposed S/T-Equalizer system, but as of the performances of the temporal equalizer alone. This is because, in part, of the hardware restriction that received signal energy can be measured only at the array output.

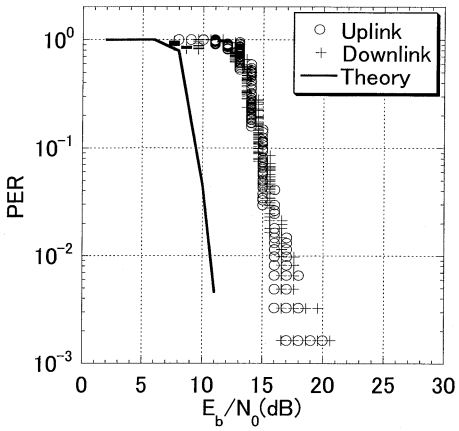

Fig. 6 PER performances at Point A.

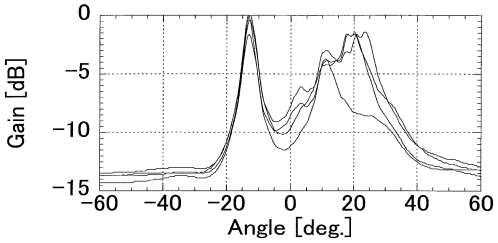

Fig. 7 Music spectrum obtained by the proposed S/T-Equalizer at Point B.

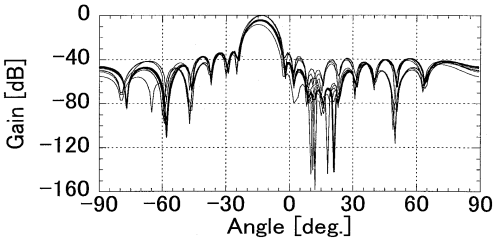

Fig. 8 Beam pattern obtained by the proposed S/T-Equalizer at Point B.

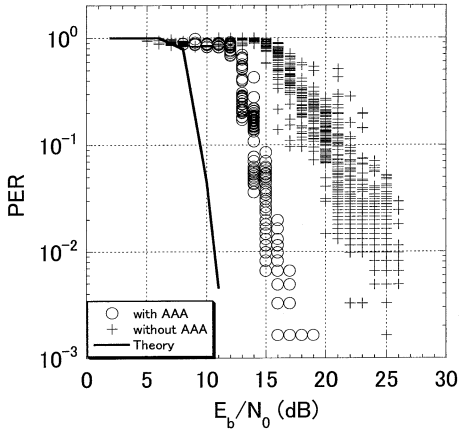

Fig. 9 Uplink PER performances at Point B.

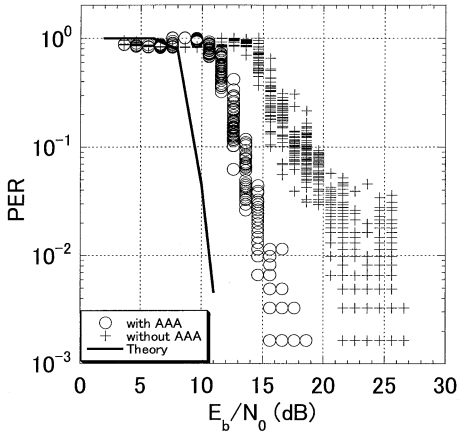

Fig. 10 Downlink PER performances at Point B.

ral equalizer at Point A was less than 1 T, and hence no BER floor is observed. Since the BER performance curve of Fig. 5 reflects bit errors occuring over periods of time during which system synchronism† is held. A more realistic performance measure is packet error rate (PER) which reflects packet errors occuring over periods of time during which the system synchronism is not held. Hence, PER is used later on to express performances of the prototyped system. Figure 6 shows at Point A PER performance and theoretical PER curves. The theoretical PER curve was obtained assuming random errors occurance over each frame. The measured PER is 5 dB worse than the theoretical curve. This is reasonable considering the impairments inherent in hardware implementation.

3.4 PER Performance under NLOS Conditions

PER performance was then evaluated when the MS was located at Points B and C, where there were no LOS paths from the BS. Figures 7 and 8 show a MUSIC spectrum and its corresponding beam pattern obtained by the prototyped system when the MS was located at Point B. In this case, three signals having DOAs of −13 degrees, 10 degrees, and 20 degrees were detected. The strongest signal of the three was the one with −14 degree DOA. Hence, the beam was steered towards that direction and the nulls were formed towards the directions of the other signals.

Figures 9 and 10 show measured uplink and downlink PER at Point B. Symbols ∘ and + represent PERs with and without AAA, respectively. In both cases, the DDFSE temporal equalizer was used. Figures 11, 12, 13 and 14 show examples of the uplink and downlink delay spread measured by the temporal equalizer at Point B

†Issues of the system synchronism includes synchronization techniques used in the receiver itself as well as that used in the auxiliary measurement system. However, detailing the synchronization mechanism is out of the scope of this papaer.

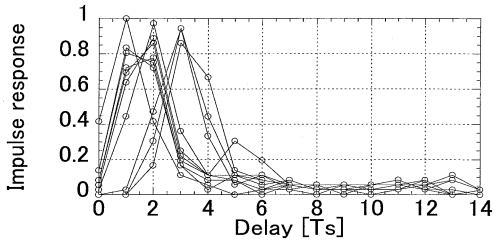

Fig. 11 Uplink impulse response with AAA at Point B.

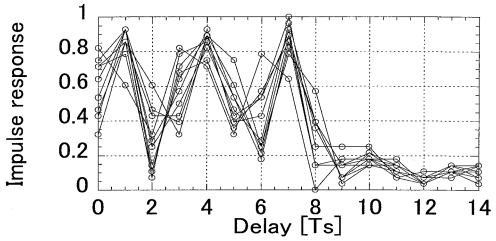

Fig. 12 Uplink impulse response without AAA at Point B.

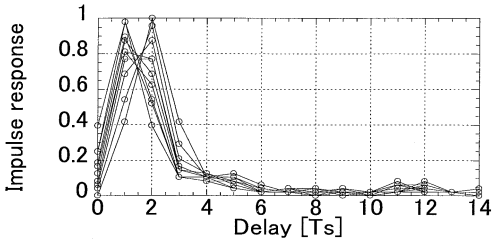

Fig. 13 Downlink impulse response with AAA at Point B.

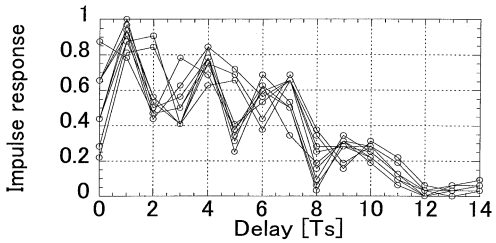

Fig. 14 Downlink impulse response without AAA at Point B.

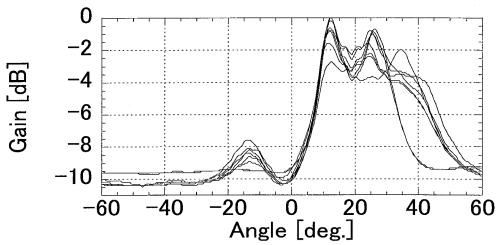

Fig. 15 Music spectrum obtained by the proposed S/T-Equalizer at Point C.

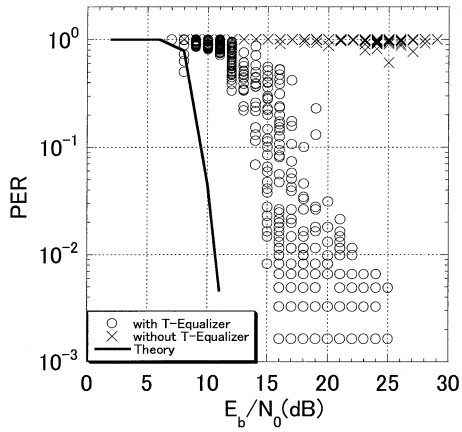

Fig. 16 Uplink PER performances at Point C.

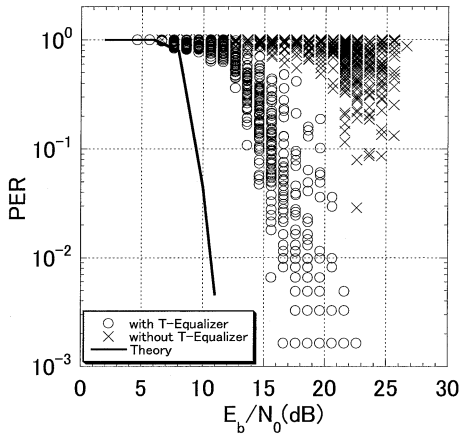

Fig. 17 Downlink PER performances at Point C.

with and without AAA, respectively. It is found that delay spread without AAA exceeds the MLSE coverage of the DDFSE equalizer. This is a major cause of degradation in the PER performance without AAA. With AAA, the delay spread can be made small enough for MLSE to cover. This improves the PER performance.

Due to the blockage from Building Y, Point C is also an NLOS region. Figure 15 shows a MUSIC spectrum obtained by the prototyped system when the MS was located at Point C. Figures 16 and 17 show measured uplink and downlink PERs when the MS was located at Point C. Symbols ∘ and × represent PERs with and without the temporal equalizer, respectively. PERs without the temporal equalizer were evaluated by coherent detection with carrier recovery using preamble sequence. In both cases, AAA was used. The delay spread estimated by the temporal equalizer was about 2.5 T. This indicates the existence of delayed components falling on the AAA's main beam, so the PER is degraded without the DDFSE temporal equalizer. The conclusion is that spatial equalization by itself can not achieve acceptable PERs if delayed desired signal components fall on the antenna's main beam.

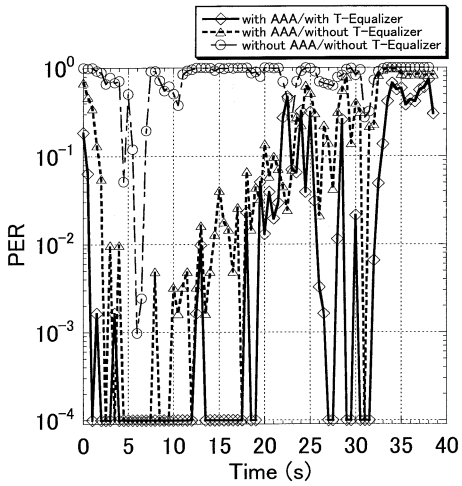

Fig. 18 Uplink PER performances at the average speed of 30 km/h.

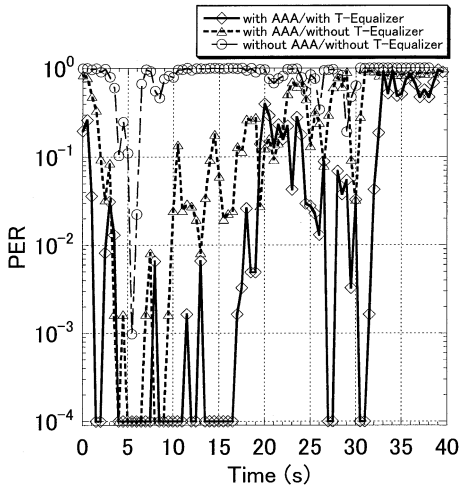

Fig. 19 Downlink PER performances at the average speed of 30 km/h.

3.5 PER Performance under Dynamic Condition

PER performance was evaluated when the MS moved from Point a to Point b as shown in Fig. 4. Figures 18 and 19 shows measured uplink and downlink PERs, respectively, for average vehicle speed of 30 km/h. The measured PERs with the proposed S/T-Equalizer, with the spatial equalizer alone, and with the temporal equalizer alone, are also plotted. For the clarity of the figures, zero PER was plotted on the 10^{-4} PER line. The MS started from Point a; it reached Point b 40 seconds later. Although the PER performance is degraded between 20 s and 25 s time points because of the NLOS condition and relatively large delay spread, the joint use of spatial and temporal equalizers can significantly improve PER performance at most of the locations over the entire 400 m measured course.

4. Conclusions

In this paper, we first proposed a new S/T-Equalizer featuring separated spatial and temporal signal processing. This separation reduces computational complexity to a practical level. A simultaneous beam and null steering AAA algorithm was derived for the S/T-Equalizer. The simultaneous beam and null steering AAA algorithm combines the concepts of beam steering and null steering: a sharp beam is steered towards the desired signal and nulls towards other signals. The proposed S/T-Equalizer was prototyped, and field tests were conducted to evaluate transmission performance of the proposed system. This paper then briefly described results of the field measurements. PER performance under NLOS and dynamic conditions suggests that the joint use of spatial and temporal equalizers can significantly improve PER performances over the case where either spatial equalizer or temporal equalizer is used alone. Performance measurement in the presence of interference is left as future study.

Acknowledgement

The authors wish to thank Mr. Kazuaki Murota, senior vice president of NTT DoCoMo, Inc. for his encouragement during this research. The authors also wish to thank Mr. Nobuhiko Miki of NTT DoCoMo, Inc. for his support in conducting field measurement.

References

[1] W. Modestio and V. Eyboglu, "Integrated multielement receiver structures for spatially distributed interference channels," IEEE Trans. IT, vol.IT-32, no.2, pp.195–219, March 1986.
[2] R. Kohno, "Spatial and temporal communication theory using adaptive antenna array," IEEE Personal Communications, pp.28–35, Feb. 1998.
[3] K. Fukawa and T. Matsumoto, "A new joint array signal processing structure and maximum likelihood sequence estimation in mobile radio communications," Smart Antenna Workshop'97, 1997.
[4] A. Duel-Hallen and C. Heegard, "Delayed decision-feedback sequence estimation," IEEE Trans. Commun., vol.37, no.5, pp.428–436, May 1989.
[5] R. Schmidt, "Multiple emitter location and signal parameter estimation," IEEE Trans. Antennas & Propag., vol.AP-34, no.3, pp.276–280, 1986.
[6] S. Applebaum, "Adaptive arrays," IEEE Trans. Antennas & Propag., vol.AP-24, no.5, pp.585–598, Sept. 1976.
[7] S.J. Orfanidis, Optimum Signal Processing, Macmillan, London, 1988.
[8] K. Fukawa and H. Suzuki, "Adaptive equalization with RLS-MLSE for frequency selective fast fading mobile radio channels," IEEE GCOM'91, pp.16.6.1–16.6.5, Phoenix, Dec. 1991.

Appendix: Derivation of Eq. (4)

Let $\boldsymbol{W}_{beam}$ and $\boldsymbol{W}_{null}$ be defined as

$$\boldsymbol{W}_{beam} = (w_{b,1}, w_{b,2}, \cdots, w_{b,m1})^T \quad (\text{A}\cdot 1)$$

and

$$\boldsymbol{W}_{null} = (w_{n,1}, w_{n,2}, \cdots, w_{n,m2})^T, \quad (\text{A}\cdot 2)$$

respectively. By using the z-transform, $\boldsymbol{W}_{beam}$ and $\boldsymbol{W}_{null}$ can be exressed in a polynomial form as

$$g_{beam}(z) = \sum_{i=1}^{m_1} w_{b,i} z^{i-1} \quad (\text{A}\cdot 3)$$

and

$$g_{null}(z) = \sum_{i=1}^{m_2} w_{n,i} z^{i-1}, \quad (\text{A}\cdot 4)$$

respectively, with z being

$$z = \exp\left(-j\frac{2\pi d}{\lambda}\sin\theta\right), \quad (\text{A}\cdot 5)$$

where d is element space and λ is wave length. The z-transform $g(z)$ of combined weight vector $\boldsymbol{W}$ is then given as a product of the two polynomials as

$$\begin{aligned} & g(z) \\ &= g_{beam}(z) \cdot g_{null}(z) \\ &= w_{b,1}w_{n,1} + (w_{b,2}w_{n,1} + w_{b,1}w_{n,2})z \\ &\quad + (w_{b,3}w_{n,1} + w_{b,2}w_{n,2} + w_{b,1}w_{n,3})z^2 + \cdots \end{aligned} \quad (\text{A}\cdot 6)$$

Coefficients of the z's terms in $g(z)$ corresponds to the (m_1+m_2-1)-element array antenna's weight vector for beam and null steering, which can be folded as Eq. (5). Obviously, this is a convolution of the vectors $\boldsymbol{W}_{beam}$ and $\boldsymbol{W}_{null}$ in Eq. (4).

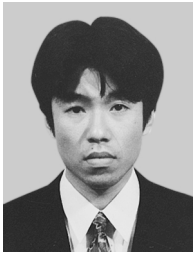

Takahiro Asai received his B.E. and M.E. degrees from Kyoto University, Kyoto, Japan, in 1995 and 1997, respectively. In 1997, he joined NTT DoCoMo, Kanagawa, Japan. Since then, he has been involved in the research of time-space signal processing for very high-speed mobile signal transmission. He is a member of the institute of electrical and electronics engineers.

Shigeru Tomisato received his B.E. degree in communication engineering from Osaka University, Osaka, Japan, in 1987. He joined Nippon Telegraph and Telephone Corporation (NTT), Japan, in 1987. Since then, he has been engaged in research on digital mobile radio communication systems. He is currently a Senior Research Engineer at NTT DoCoMo, Inc., Kanagawa-ken, Japan.

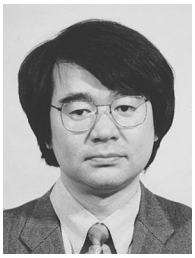

Tadashi Matsumoto received his B.S., M.S., and Ph.D. degrees in electrical engineering from Keio University, Yokohama, Japan, in 1978, 1980, and 1991, respectively. He joined Nippon Telegraph and Telephone Corporation (NTT) in April 1980. From April 1980 to May 1987, he was involved in the research of signal transmission technologies such as modulation/demodulation schemes, as well as radio link design for mobile communications systems. He participated in the R&D project of NTT's high capacity mobile communications system where he was responsible for the development of the base-station transmitter/receiver equipment for the system. From May 1987 to February 1991, he studied error control strategies such as forward error correction, trellis-coded modulation, and automatic repeat request in digital mobile radio channels. He developed an efficient new automatic repeat request scheme suitable to the error occurrence in TDMA mobile signal transmission environments. He was involved in the development of a Japanese TDMA digital cellular mobile communications system. He led the development of the facsimile and data communications service units for the system. In July 1992, he transferred to NTT DoCoMo, Inc., Kanagawa, Japan. From February 1991 to April 1994, he intensively studied multiuser detection schemes for multipath mobile communications environments. He also concentrated on the research of a maximum *a posteriori* probability (MAP) algorithm and its reduced complexity version for decoding concatenated codes. From 1992 to 1994, he served as a part-time lecturer at Keio University. In April 1994, he moved to NTT America, where he served as Senior Technical Advisor of the joint project with NTT and NEXTEL Communications. In March 1996, he returned to NTT DoCoMo. Since then, he has been conducting research on time-space signal processing for very high-speed mobile signal transmission. Presently, he is an Executive Research Engineer at NTT DoCoMo. He is a senior member of the Institute of Electrical and Electronics Engineers.